Korea-Australia Rheology Journal
Vol. 19, No. 3, November 2007 pp. 141-146

Tethered DNA shear dynamics in the flow gradient plane: application to double tethering

Christopher A. Lueth and Eric S. G. Shaqfeh[1]*
Department of Chemical Engineering, Stanford University, Stanford, California 94305
[1]Departments of Chemical Engineering and Mechanical Engineering, Stanford University, Stanford, California 94305.
(Received Septeber 16, 2007)

Abstract

We examine the wall contact of a 3 μm tethered DNA chain's free end under shear with a focus on developing schemes for double-tethering in the application of making scaffolds for molecular wires. At this scale our results are found to be highly dependent on small length scale rigidity. Chain-end-wall contact frequency, mean fractional extension deficit upon contact, and standard deviation in extension upon contact are examined for scaling with dimensionless flow strength, Wi. Predictions made using a one dimensional approximation to the Smoluchowski equation for a dumbbell and three dimensional dumbbell simulations produce extension deficit, standard deviation, and frequency scaling exponents of $-1/3$, $-1/3$, and $2/3$, respectively whereas more fine-grained Kratky-Porod (KP) simulations produce scaling exponents of -0.48, -0.42, and 0.76. The contact frequency scaling of 2/3 is derived from the known results regarding cyclic dynamics Analytical scaling predictions are in agreement with those previously proposed for λ-DNA. [Ladoux and Doyle, 2000, Doyle et al., 2000]. Our results suggest that the differences between the dumbbell and the KP model are associated with the addition of chain discretization and the correct bending potential in the latter. These scaling results will aide future exploration in double tethering of DNA to a surface.

Keywords : tethered DNA, flow gradient plane, Weissenberg number scaling, Kratky-Porod

1 Introduction

Recent successes in DNA metallization [Braun et al., 1998] have inspired a variety of new applications utilizing DNA as molecular wires. One such application is the use of metallized DNA as electrical contacts to organic single molecules, allowing for the study of the electrical properties of single molecules and providing tremendous information toward the growing field of "plastic electronics." In this context, we are referring to the synthesis of a DNA-organic molecule-DNA sandwich (DOD) followed by subsequent stretching and double-tethering of the DOD between two gold electrodes. Metallization of the DNA completes the molecular circuit. Flow processing has been suggested as a means of stretching and orienting these DOD bridges between electrodes [Braun et al., 1998] and these bridges are typically between $1-3$ μm in total length. For example, one can first tether one end to an electrode, stretch the free end with shear flow, and then tether the free end to a second electrode. Thus precise control of tethered DNA chains subjected to shear flow is desired to repeatably create these DOD bridges.

In the present manuscript, the detailed dynamics of a DNA chain in flow are examined through scaling arguments and simulations in the flow-gradient plane. Using Brownian Dynamic simulations of wormlike-chains, we have developed a statistical description of the contact of a wall-tethered 3 μm (22 Kuhn Step) DNA chain's free end with the wall. Specifically, we will determine how chain-wall contact frequency, mean fractional extension deficit upon contact, and the standard deviation in extension upon contact scale with flow strength. Ultimately, our results will afford precise control over the creation of DNA bridges.

Stretching of tethered polymer chains subject to shear flow has been studied via simulation in weak flows [Schroeder et al., 2005] and for both weak and strong flows focusing on the flow-vorticity plane [Ladoux and Doyle, 2000, Doyle et al., 2000]. Fluorescent microscopy experiments performed by Doyle introduced the idea of cyclic dynamics of tethered DNA chains under weak flows. Schroeder, with the aide of Brownian dynamics simulations, demonstrated the presence of a characteristic frequency for cyclic motion of a tethered polymer in shear flow when $1 < Wi < 10$, where the Weissenberg number, Wi, is the shear rate times the longest polymer relaxation time.

Ladoux and Doyle performed fluorescent microscopy experiments and Brownian dynamics bead-spring simulations for 21, 42, and 63 μm DNA chains. They showed

*Corresponding author: esgs@stanford.edu
© 2007 by The Korean Society of Rheology

that the mean extension deficit, the extension in the flow direction subtracted from the chain contour length, of a tethered DNA chain scales with $Wi^{-1/3}$. For freely jointed chains, they predicted mean extension deficit scaling of $Wi^{-1/2}$.

All experiments to date included examinations of chain dynamics in the flow-vorticity plane, affording no insight into chain dynamics very near the wall or in the flow-gradient plane. Previous simulations consist of strictly bead-spring simulations which may not capture the appropriate dynamics for short DNA segments. It is believed that chain-end-wall contact dynamics are highly dependent on the bending modulus of a short semiflexible chain. Taking this into consideration, Brownian dynamic simulations in the shear flow-gradient plane using semiflexible Kratky-Porod chains [Kratky and Porod, 1949] are required to fully resolve chain-end-wall contact statistics.

2. Models

2.1. Dumbbell Approximation

Bead-rod and bead-spring models are employed in subsequent sections to study tethered chain dynamics near a wall. However, in order to derive scaling arguments, a simpler model may be used including representing the chain as a single, freely draining spring tethered to the wall. Similar methods have been utilized in nonlinear [Beck and Shaqfeh, 2006] flows. The probability density, Ψ, of the spring's free end is given by the Smoluchowski equation [Bird et al., 1987]:

$$\frac{\partial \Psi}{\partial t}+\frac{\partial}{\partial \mathbf{R}}\cdot\left(\frac{\partial \mathbf{u}^{\infty}}{\partial \mathbf{x}}\cdot\mathbf{R}\Psi\right)-\frac{1}{\zeta}\frac{\partial}{\partial \mathbf{R}}\cdot\left(Hf\left[\frac{\mathbf{R}}{L}\right]\mathbf{R}\right)=D\frac{\partial}{\partial \mathbf{R}}\cdot\frac{\partial \Psi}{\partial \mathbf{R}} \quad (1)$$

where $\mathbf{R}$ represents the position of the spring's end; $\frac{\partial \mathbf{u}^{\infty}}{\partial \mathbf{x}}$ is the rate of strain tensor; and the third term in the equation represents the entropic spring force, which will be described in further detail later. The diffusion coefficient, D, of the bead representing the chain end is defined as $\frac{k_BT}{\zeta}$, where k_BT is the thermal energy of the fluid and ζ is the bead drag coefficient of the end bead.

2.2. The Bead Spring Chain Model

The dumbbell model is useful for analytical work and for scaling arguments, but if internal modes of the chain bring important new physics a bead spring model can be used. In this case, the polymer chain is modeled by a series of Brownian particles held together by entropic springs. Ermak and McCammon [Ermak and McCammon, 1978] developed an equation for the spatial evolution of hydrodynamically interacting Brownian particles under constraining forces. For 150 Kuhn step λ-DNA, it has been shown that hydrodynamic interactions are rather insignificant in shear and extensional flow [Hsieh et al., 2003]; therefore, it follows that for a 22 Kuhn step chain far from equilibrium, hydrodynamic interactions can be safely neglected. A system of stochastic differential equations describing the positions, $\mathbf{R}$, of freely draining interacting beads, $i=1, 2, \ldots N$, is as follows [Öttinger, 1996]:

$$d\mathbf{R}_i=\begin{cases} 0; & i=0 \\ \left(\mathbf{u}_i^{\infty}+\frac{1}{\zeta}(\mathbf{F}_i^{W}+\mathbf{F}_i^{s}-\mathbf{F}_{i-1}^{s})\right)dt+\sqrt{\frac{2k_BT}{\zeta}}d\mathbf{W}_i; & i=2;N-1 \\ \left(\mathbf{u}_i^{\infty}+\frac{1}{\zeta}(\mathbf{F}_i^{W}+\mathbf{F}_{N-1}^{s})\right)dt+\sqrt{\frac{2k_BT}{\zeta}}d\mathbf{W}_i; & i=N \end{cases} \quad (2)$$

This results from a balance between disturbances caused by the free stream velocity, $\mathbf{u}_i^{\infty}$; a short range wall exclusion force, $\mathbf{F}_i^{W}$; the entropic spring force from spring i, $\mathbf{F}_i^{S}$; and solvent-bead collisions expressed as an isotropic Weiner process, $d\mathbf{W}_i$ [Öttinger, 1996]. Each spatial component of $d\mathbf{W}_i$ is modeled as a Gaussian random number with a variance of dt [Somasi et al., 2002]. The first bead in the chain is tethered to the wall and accordingly has no net disturbance. Note that while this model captures the correct extensional force of the worm-like chain using the appropriate spring force $\mathbf{F}_i^{S}$ as discussed below, it does not capture the appropriate bending modulus over the length of the chain [Bustamante et al., 1994, Marko and Siggia, 1995].

The only non zero component of the free stream velocity is defined to be that for flow in the x-direction, whereas the wall normal is defined to be in the y-direction, resulting in $\mathbf{u}_i^{\infty}=\dot{\gamma}[y, 0, 0]$, where $\dot{\gamma}$ is the shear rate.

The wall exclusion force is a non-physical interaction used only to prevent the bead from penetrating the wall. Ideally, this potential should be infinitely large at the wall and have a very short range of influence. However, due to simulation convergence issues and the use of a fixed time step, we employ the interaction used elsewhere [Beck and Shaqfeh, 2006, Jendrejack et al., 2004]:

$$\mathbf{F}_i^{W}=\begin{cases} C_{\mathrm{W}}\frac{k_BT}{b_k}\left(\frac{y_i}{\delta_{\mathrm{W}}}-1\right)^2\mathbf{n}; & y_i<\delta_{\mathrm{W}} \\ 0; & y_i\geq\delta_{\mathrm{W}} \end{cases} \quad (3)$$

where $\mathbf{n}=[0, 1, 0]$ is the vector normal to the wall and y_j is the distance between bead j and the wall. The constant W is the boundary thickness of the wall force, chosen to be equal to twice the standard deviation of the Brownian disturbance, $\delta_W=2\sqrt{\frac{2k_BT}{\zeta}dt}$, to ensure that a Brownian fluctuation will not force a bead through the wall with 95% confidence. The strength of the wall force, $C_W=25$, was chosen to prevent the bead from penetrating the wall on a frequent basis [Beck and Shaqfeh, 2006, Jendrejack et al.,

2004]. The time step, $dt=10^{-5}$, is chosen such that $\delta_W << R_g$, where R_g is the radius of gyration for the entire chain, and thus the wall force has a negligible effect on the wall contact dynamics.

The wormlike chain force law [Bustamante et al., 1994, Marko and Siggia, 1995] is used for the entropic spring force between consecutive beads in the chain.

$$\mathbf{F}_i^S = Hf\left[\frac{Q_i}{L}\right]\boldsymbol{Q}_i,$$

$$f\left[\frac{Q_i}{L}\right] = \frac{L}{6Q_i}\left(\frac{1}{(1-Q_i/L)^2} - 1 + 4\frac{Q_i}{L}\right) \tag{4}$$

The force constant, $H=\frac{3k_BT}{N_{ks}b_k^2}$, where N_{ks} is the number of Kuhn steps per spring, bk is the length of a Kuhn step, and the connecter vector, $\boldsymbol{Q}_i=\mathbf{R}_{i+1}-\mathbf{R}_i$, has magnitude, Q_i, which is smaller than the maximum extension, L, of the spring.

2.3. Kratky-Porod Chain

In order to elucidate chain end dynamics near the wall, one may use a more fine grained model. The appropriate model is a modified version of the Kramer's feely-jointed bead rod chain model [Kramers, 1956] including the bending modulus, i.e. the Kratky-Porod model [Kratky and Porod, 1949]. This is the model from which the wormlike spring law, equation (4) is derived [Marko and Siggia, 1995]. The polymer chain is represented by a bead-rod chain with more segments, $N-1$, than Kuhn steps, N_k. This way it is possible to allow the bending modulus to control the persistence length regardless of the discretization of the chain [Öttinger, 1996].

A balance of the hydrodynamic force, the wall force, bending constraint forces, rod tensions, and the Brownian force results in:

$$d\mathbf{R}_i = \left(\mathbf{u}_i^\infty + \frac{1}{\zeta}(\mathbf{F}_i^W + \mathbf{F}_i^C + \mathbf{F}_i^T)\right)dt + \sqrt{\frac{2k_BT}{\zeta}}d\mathbf{W}_i \tag{5}$$

The tension forces, needed to keep the rod lengths fixed, are unknown *a priori* and are calculated iteratively using Picard's method [Liu, 1989, Somasi et al., 2002] until the following constraint is satisfied:

$$||\mathbf{R}_{i+1}-\mathbf{R}_i|-l| < \varepsilon \tag{6}$$

where l is the length of the discretized rod segment and ε is chosen to be $l*10^{-6}$.

A stiffer wall force,

$$\mathbf{F}_j^W = C_W k_B T\left(\frac{1}{\exp[5h_j/\delta_W]-1} - \frac{1}{\mathrm{ewp}[5]-1}\right)\mathbf{n}; \quad h_j < \delta_W$$

$$0; \quad h_j \geq \delta_W \tag{7}$$

than previously used for the bead-spring model can be implemented with the addition of an adaptive time step algorithm. This will help improve the dynamics of the chain end very near the wall. The boundary thickness is again chosen to be very small, $\delta_W=0.03l=\frac{1}{100}R_g$, and C_W is chosen to be comparable to other bending and tension forces.

Discretization of the bending force for a continuous chain yields,

$$\frac{\hat{l}_P}{l}k_BT(-\mathbf{R}_{i-2}+4\mathbf{R}_{i-1}-6\mathbf{R}_i+4\mathbf{R}_{i+1}-\mathbf{R}_{i+2}); \quad 3\leq i\leq N-2$$

$$\mathbf{F}_i^C = \frac{\hat{l}_P}{l}k_BT(2\mathbf{R}_{i+1}-5\mathbf{R}_i+4\mathbf{R}_{i\pm1}-\mathbf{R}_{i\pm2}); \quad i=2(top),\ N-1(bot) \tag{8}$$

$$\frac{\hat{l}_P}{l}k_BT(-\mathbf{R}_i+2\mathbf{R}_{i\pm1}-\mathbf{R}_{i\pm2}); \quad i=2(+),\ N-1(-)$$

where $\hat{l}_P$ is the persistence length of the chain in the limit of infinite bead number [Yamakawa, 1971, Evans, 1995]. For finite chains, the actual persistence length, l_P , can be calculated by fitting the simulation results for the chain tangent correlation function.

$$\langle \mathbf{Q}_i \cdot \mathbf{Q}_1 \rangle = \exp\left[-\frac{(i-1)l}{l_P}\right] \tag{9}$$

Thus, the actual persistence length of the chain is known and N or l_P is determined iteratively to reproduce the appropriate number of Kuhn steps.

3 Results and Discussion

3.1. Dumbbell Predictions

To examine the flow strength scaling of the extension, the variance in extension, and the frequency of chain-end contact with the wall, we begin with the dimensionless form of equation 1.

$$\frac{\partial\Psi}{\partial\tau} + \frac{\partial}{\partial\mathbf{r}}\cdot(Wi\kappa\mathbf{r}\Psi - f[r]\mathbf{r}\Psi) = \frac{1}{3N_k}\frac{\partial}{\partial\mathbf{r}}\cdot\frac{\partial\Psi}{\partial\mathbf{r}} \tag{10}$$

in dimensionless variables $\mathbf{r}=\mathbf{R}/L$ and $\tau=tH/\zeta$ and including the dimensionless parameters: the Weissenberg number, $Wi=\dot{\gamma}\zeta/H$, and the number of Kuhn steps in the entire chain, N_k. To further simplify the problem, the chain is assumed to be near maximum extension for strong flows. Therefore, the spring force asymptotically approaches

$$f \approx \frac{1}{6(1-x)^2} \tag{11}$$

Integrating equation 10 over the vorticity direction, z, followed by integration over the flow direction, x, produces, with overbar defined as: $\bar{\cdot} = \int_0^\infty\int_0^\infty \cdot\, dzdx$

$$\frac{\partial\bar{\Psi}}{\partial\tau}=\frac{\partial}{\partial y}\left(\frac{1}{3N_k}\frac{\partial\bar{\Psi}}{\partial y}+\overline{\frac{y}{6(1-x)^2}\Psi}\right) \tag{12}$$

To eliminate any dependence on x in equation 12, we balance the flow force and the spring force in the flow direction, $Wi\, y\approx\frac{x}{6(1-x)^2}$, and thus calculate the first term in an expansion around $(1-x)=0$. This results in $y\approx\frac{x}{6Wi(1-x)^2}$ $\approx\frac{1}{6Wi(1-x)^2}$, and substituting into equation 12 yields:

$$\frac{\partial\bar{\Psi}}{\partial\tau}=\frac{\partial}{\partial y}\left(\frac{1}{3N_k}\frac{\partial\bar{\Psi}}{\partial y}+Wiy^2\bar{\Psi}\right) \tag{13}$$

thus, at steady state a solution of the following form can be derived:

$$\bar{\Psi}=\frac{3(Wi\,N_k)^{1/3}}{\Gamma[1/3]}\exp[-Wi\,N_k y^3] \tag{14}$$

This approximate probability density function enables the calculation of average properties, $\langle\cdot\rangle=\int_0^\infty\int_0^\infty\int_0^\infty\cdot\,dxdydz$, to yield the scalings:

$$\langle y\rangle\sim Wi^{-1/3}N_k^{-1/3}$$
$$\langle y^2\rangle\sim Wi^{-2/3}N_k^{-2/3} \tag{15}$$

and returning to our approximation, $y\approx 1/6Wi(1-x)^2$, or $\langle y\rangle\sim 1/Wi\langle 1-x\rangle^2\sim 1/Wi\langle(1-x)^2\rangle$, we find:

$$\langle 1-x\rangle\sim Wi^{-1/3}N_k^{1/6}$$
$$\sigma_x\sim Wi^{-1/3}N_k^{1/6} \tag{16}$$

These results are in agreement with the Wi scalings derived by Ladoux et. al. [Ladoux and Doyle, 2000].

When analyzing the frequency at which the chain-end contacts the wall, we first re-examine the 1-D Smoluchowski equation, equation 13. If we assume an initial stretched chain at a distance y_0 from the wall, there are diffusive and entropic spring processes driving the chain end to the wall. The time-dependent equation 13 can not be solved analytically, but since the equilibrium distribution is derived by balancing these two processes, scalings can be found by assuming a purely diffusive process. The diffusion equation then implies that the time it takes to diffuse to the wall is:

$$\tau\approx\frac{y_0^2}{2\frac{1}{3N_k}} \tag{17}$$

and, assuming the distribution for y_0 in equation 14, the frequency of chain-end contact scales as

$$f\sim Wi^{2/3}N_k^{-1/3} \tag{18}$$

This argument is equivalent to saying that the frequency of wall contact is proportional to the inverse time that a stretched chain takes to diffuse a distance $\langle y^2\rangle\sim Wi^{-2/3}N_k^{-2/3}$

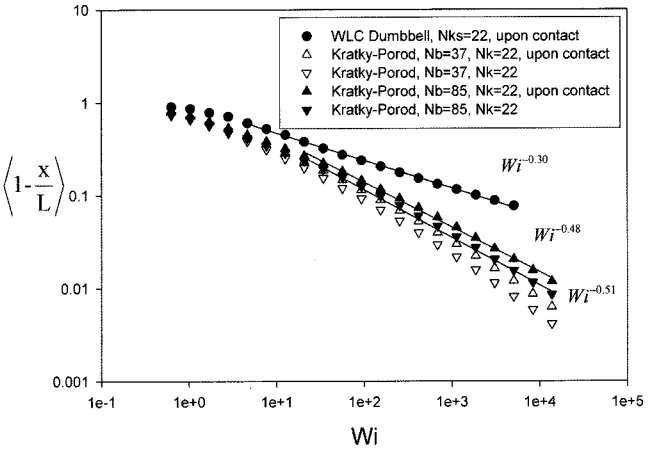

Fig. 1. Kratky-Porod and dumbbell simulation results for dimensionless extension deficit and deficit upon wall contact versus Wi for 22 Kuhn step wormlike chains. Kratky-Porod chains consisting of 37 and 85 beads require an $\frac{\tilde{l}_P}{l}$ of 1 and 2.5, respectively, to reproduce 22 Kuhn steps. Solid lines represent least square fits to the asymptotic behavior.

and thus is consistent with the original of Doyle and coworkers [Ladoux and Doyle, 2000, Doyle et al., 2000].

3.2. Simulations

Simulation results are compared to predictions for wall-contact parameter scaling with Wi for 22 Kuhn step chains. Bead contact is defined as the point at which the distance from the wall is less than δ_W. The Weissenberg number is a measure of the flow strength relative to the polymer relaxation time: $Wi=Pe\lambda$, where λ is the dimensionless, longest polymer relaxation time calculated by 30% extension relaxation [Hsieh et al., 2003, Beck and Shaqfeh, 2006]. All simulations are run for 22 Kuhn step chains. A commonly accepted condition for the bead spring model is $N_{ks} > 10$ [Somasi et al., 2002]. This limits our simulations to one or two springs when modeling a 22 Kuhn step chain. Extension results were found to be similar for these two cases and only results for dumbbell simulations are presented.

Fig. 1 shows a plot of the extension deficit, $\langle 1-x/L\rangle$, versus Weissenberg number, Wi. It is apparent that the scaling prediction of $Wi^{-1/3}$, derived from the 1-D Smoluchowski approximation in the previous section, agrees well with dumbbell simulations. The slight underprediction in the scaling factor for extension deficit upon wall contact, -0.30, is most likely caused by the deficiency of the approximation, $y\approx\frac{x}{6Wi(1-x)^2}$ near the wall, as shown in Fig. 4. This inconsistency facilitates chain-end-wall contact at higher extensions during simulations, as shown by the higher probability density to the left of the solid line in Fig. 4.

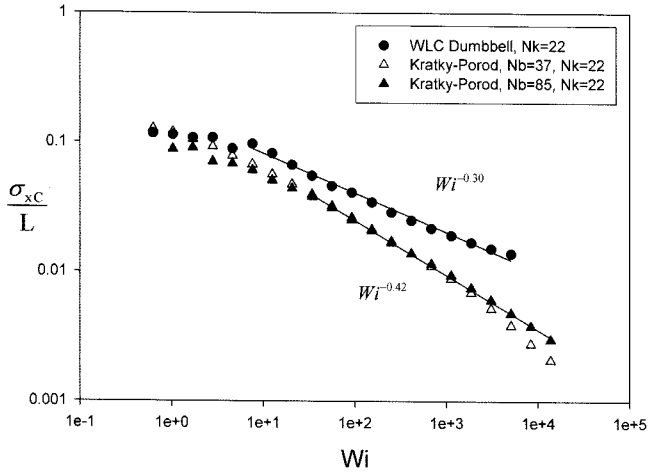

Fig. 2. Kratky-Porod and dumbbell simulation results for the standard deviation in dimensionless extension upon wall contact versus Wi for chains of length N_k=22. Kratky-Porod chains consisting of 37 and 85 beads require an $\frac{\hat{l}_P}{l}$ of 1 and 2.5, respectively, to reproduce 22 Kuhn steps. Solid lines represent least square fits to the asymptotic behavior.

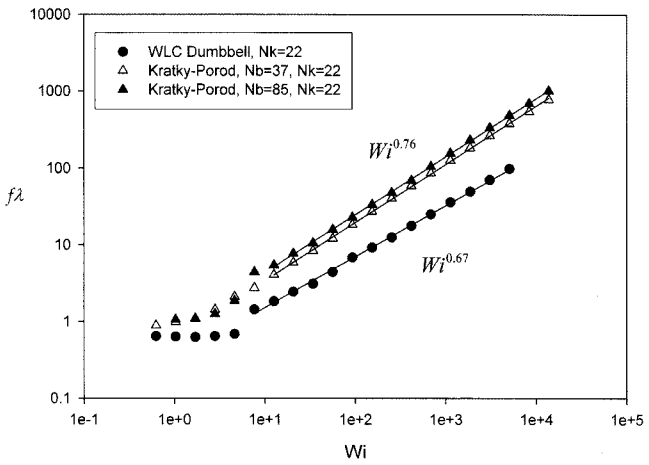

Fig. 3. Kratky-Porod and dumbbell simulation results for the dimensionless frequency of chain end-wall contact versus Wi. Kratky-Porod chains consisting of 37 and 85 beads require $\frac{\hat{l}_P}{l}$ of 1 and 2.5, respectively, to reproduce 22 Kuhn steps. Solid lines represent least square fits to the asymptotic behavior.

This shift of the probability density to the left is more important at smaller Wi than it is at larger Wi, which causes an overprediction in the extension deficit scaling with Wi at the wall. However, Kratky-Porod simulations apparently yield a very different scaling for extension deficit of $Wi^{-0.51}$ and extension deficit upon wall contact of $Wi^{-0.48}$. This discrepancy is most likely a result of either the increased refinement of the chain or the addition of a wormlike bending potential. The figure shows Kratky-Porod simulations for discretizations of 37 and 85 beads. Fewer number of beads will produce results between freely-jointed chain results and wormlike chain results. As the number of discretization points increase, results will approach those of the wormlike chain.

The bending potential and refinement of the Kratky-Porod model also seem to affect the standard deviation of extension upon contact. Fig. 2 shows that dumbbell simulations yield the predicted $Wi^{-1/3}$ scaling, whereas Kratky-Porod simulations produce a $Wi^{-0.42}$ scaling consistent with the extension deficit scaling. With the addition of a bending potential it becomes exceedingly difficult for the chain end to diffuse as the chain extends, limiting the fluctuations in length upon contact. As a result, the scaling exponent becomes more negative. Our predictions for frequency of bead-chain contact scaling of $Wi^{2/3}$ agrees with our dumbbell simulations as shown in Fig. 3. The Kratky-Porod simulations produce a different scaling of $Wi^{0.76}$. This supports previous statements that increased discretization plays an important role in chain-end-wall contact. The diffusivity of the chain end is higher than that of an element within the chain and as the chain itself gets closer

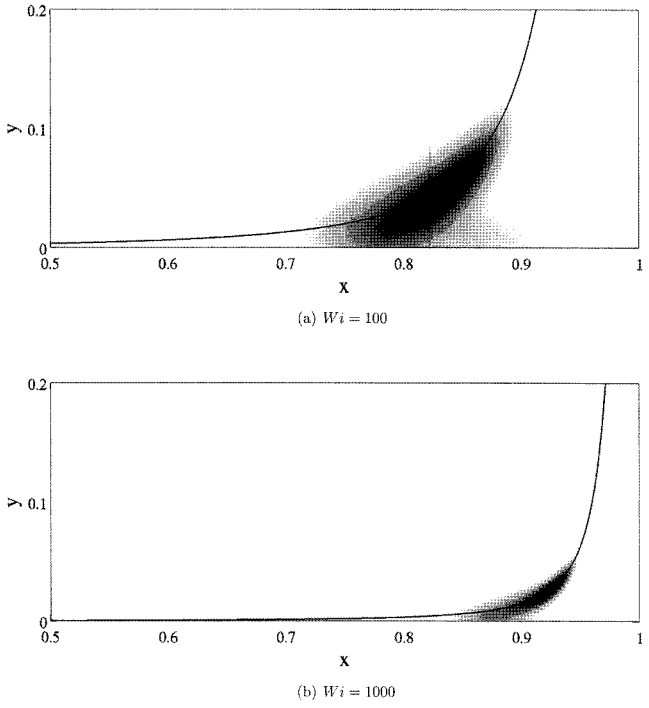

Fig. 4. Comsol numerical solutions to 2-D Smoluchowski equation, the precursor to equation 12 before x has been integrated out, with the solid line representing the contour of $y=\frac{x}{6Wi(1-x)^2}$. Calculations use $\frac{1}{3N_k}=0.015$, correlating to a 22 Kuhn step chain, and Wi of (a) 100 and (b) 1000.

to the wall, it becomes increasingly easier for the chain end to contact the wall. Dumbbell predictions were made assuming the diffusivity of the chain end was equal to that

of half the chain. The addition of a chain bending potential should counteract this effect, because diffusion perpendicular to the chain should decrease. It is important to note that experiments performed by Ladoux and Doyle on tethered 21, 42, and 63 μm λ-phage DNA in shear flow [Ladoux and Doyle, 2000] show that mean extension deficit scales with $Wi^{-1/3}$, which is in agreement with their and our present theoretical predictions for bead-spring models. Therefore it is reasonable to conclude that, either the added bending potential only plays a large role in modeling short chain end dynamics at the wall, or the scaling deviation is only apparent for higher Wi than those examined by Ladoux and Doyle.

4. Conclusion

When double tethering a DNA chain to a surface, it is important to understand the free-chain-end dynamics of a single-end-tethered DNA chain under shear flow. It is clear that the wormlike chain entropic spring model is insufficient when modeling chain-end-wall contact statistics in shear flow at least for small chains. Chain discretization and a bending potential along the chain play an important role in wall contact statistics. The wormlike chain entropic spring model is capable of correctly simulating averaged properties involving dynamics away from the wall [Ladoux and Doyle, 2000] for large chains, but more refinement is needed when considering dynamics very near the wall. Dumbbell simulations produce scalings for extension deficit upon wall contact, standard deviation of extension upon wall contact, and wall contact frequency of: $<1-x>_c \sim Wi^{-0.3}$, $<\sigma_x>_c \sim Wi^{-0.3}$, and $f \sim Wi^{0.67}$, respectively. By comparison, Kratky-Porod simulations produce scalings of: $<1-x>_c \sim Wi^{-0.48}$, $<\sigma_x>_c \sim Wi^{-0.42}$, and $f \sim Wi^{0.76}$, respectively, for a 22 Kuhn step chain.

Further study is needed for freely jointed chains, to test whether the disparity in scaling for wall-contact statistics between dumbbell and Kratky-Porod models is due to the addition of chain refinement or the addition of the correct bending potential.

Acknowledgment

This work has been supported by the Nanoscale Interdisciplinary Research Team, a National Science Foundation funded organization.

References

Beck, V. A. and E. S. G. Shaqfeh, 2006, Ergodicity breaking and conformational hysteresis in the dynamics of a polymer tethered at a surface stagnation point, *J. Chem. Phys.* **124**, 094902.

Bird, R. B., Curtiss, C. F., Armstrong, R. C., and O. Hassager, 1987, *Dynamics of Polymeric Liquids*, volume **2**. Wiley, New York.

Braun, E., Y. Eichen, U. Sivan, and G. Ben-Yoseph, 1998, DNA-templated assembly and electrode attachment of conducting silver *wire. Nature* **391**, 775-778.

Bustamante, C., J. F. Marko, E. D. Siggia, and S. Smith, 1994, Entropic elasticity of λ-phage DNA, *Science* **265**, 1599-1600.

Öttinger, H. C., 1996, *Stochastic Processes in Polymer Fluids*, Springer.

Doyle, P. S., B. Ladoux, and J. L. Viovy, 2000, Dynamics of a tethered polymer in shear flow, *Physical Review Letters* **84**, 4769-4772.

Ermak, D. L. and J. A. McCammon, 1978, Brownian dynamics with hydrodynamic interactions. *J. Chem. Phys.* **69**, 1352-1360.

Evans, A. R. 1995, *An experimental and theoretical investigation of polymer conformation during flow through a dilute fiber bed*, PhD thesis, Stanford University.

Hsieh, C. C., L. Li, and R. G. Larson, 2003, Modeling hydrodynamic interaction in brownian dynamics: simulations of extensional flows of dilute solutions of DNA and polystyrene, *J. Non-Newtonian Fluid Mech.* **113**, 147-191.

Jendrejack, R. M., D. C. Schwartz, J. J. de Pablo, and M. D. Graham, 2004, Shear-induced migration in flowing polymer solutions: simulation of long-chain DNA in microchannels, *J. Chem. Phys.* **120**, 2513.

Kramers, H. A. 1956, *Collected Scientific Papers*, North-Holland Publishing Co.

Kratky, O. and G. Porod, 1949, Röntgenuntersuchung gelöster fadenmoleküle. *Rec. Trav. Chim.* **68**, 1106.

Ladoux, B. and P. S. Doyle, 2000, Stretching tethered DNA chains in shear flow, *Europhysics Letters* **52**, 511-517.

Liu, T. W., 1989, Flexible polymer chain dynamics and rheological properties in steady flows, *J. Chem. Phys.* **90**, 5826-5842.

Marko, J. F. and E. D. Siggia, 1995, Stretching DNA, *Macromolecules* **28**, 8759-8770.

Schroeder, C. M., R. E. Teixei, E. S. G. Shaqfeh, and S. Chu, 2005, Characteristic periodic motion of polymers in shear flow, *Physical Review Letters* **95**, 018301.

Somasi, M., B. Khomami, N. J. Woo, J. S. Hur, and E. S. G. Shaqfeh 2002, Brownian dynamics simulations of bead-rod and bead-spring chains: numerical algorithms and coarse-graining issues, *J. Non-Newtonian Fluid Mech.* **108**, 227-255.

Yamakawa, H., 1971, *Modern Theory of Polymer Solutions*, Harper & Row.